Sensitive Luminescent Chemosensing of Fluoride based on Eu-doped Zn-LMOF in Aqueous Media. Structural and Spectroscopic Studies

Paola Toledo-Jaldín,[a,d*] Cristian Pinzón-Vanegas,[b] Juan Pablo León-Gómez,[b] Alien Blanco Flores,[a] Diego Martínez-Otero,[c] Iván A. Reyes Domínguez,[d] Daniel Canseco-González,[e] Luis D. Rosales-Vázquez,[b] María K. Salomón-Flores[b] and Alejandro Dorazco-González[b*]

[a] *Technological Superior Studies Tianguistenco, Mechanical Engineering, Santiago Tianguistenco 52650, México.*
[b] *Institute of Chemistry, National Autonomous University of Mexico, Mexico City 04510.*
[c] *Centro Conjunto de Investigación en Química Sustentable UAEM-UNAM, Instituto de Química, Universidad Nacional Autónoma de México, Toluca 50200 Estado de México, México.*
[d] *Autonomous University of San Luis Potosi, Institute of Metallurgy, San Luis Potosi 78210, México*
[e] *CONACYT-Laboratorio Nacional de Investigación y Servicio Agroalimentario y Forestal, Universidad Autónoma Chapingo, Texcoco de Mora CP 56230*
Corresponding authors: helenpao27@hotmail.com, adg@unam.mx

Electronic Supporting Information

Table S1 Crystal data and structure refinement for **Zn-LMOF**.

Table S2 Selected bond distances (Å) and angles (°) around Zn atoms.

Table S3 Analytical parameters of recent luminescent materials for F^- sensing in aqueous media.

Fig. S1 Emission spectra for **$Eu_{3\text{-}24\%}$@Zn-LMOF**.

Fig. S2 3D diagram from crystal structure of **Zn-LMOF**.

Fig. S3 Simulated and experimental powder X-ray diffraction patterns of **Zn-LMOF**.

Fig. S4 TGA curve of **Zn-LMOF**.

Fig. S5 ^{13}C ss-CPMAS NMR (spinning rate at 8 kHz) spectrum for **Zn-LMOF**.

Fig. S6 Solid-state excitation and emission spectra of compound **Zn-LMOF**.

Fig. S7 Excitation spectrum of **Eu@Zn-LMOF** at room temperature by monitoring the Eu(III) ions (616 nm).

Fig. S8 ATR-FTIR spectra to assess the **Eu@Zn-MOF** hydrostability.

Fig. S9 Calibration curves with linear fit at 616 nm (λ_{ex}= 260 nm) of **Eu@Zn-LMOF** dispersed in EtOH–H2O (v/v, 8/2) by adding F^- ions with (□) and without (■) interfering anions (1.0 mM each).

Fig. S10 IR spectra of as-synthesised **Zn-LMOF** and, **Eu@Zn-LMOF** treated with NaF for 12 h.

Fig. S11 SEM-EDS **Eu@Zn-LMOF** after F^- detection.

General Considerations

Materials and methods

All reagents and reactants were purchased directly by commercial approach and were used without any purification. The raw materials were $Zn(NO_3)_2 \cdot 6H_2O$ (Aldrich, 98%), benzene-1,4-dicarboxylic acid (Aldrich, ≥98%), $EuCl_3 \cdot 6H_2O$ (Aldrich, 99.9%), *N*,*N*-dimethylformamide, (99%) methanol (Tecsiquim, 99.8%), ethanol (Tecsiquim, 99.8%), dimethyl formamide (Aldrich, 99.8%), acetonitrile (Tecsiquim, ≥99.5%), butanol (Tecsiquim, ≥99.4%), carbon tetrachloride (Tecsiquim, >99%), chloroform (Tecsiquim, 99.7%), dichloromethane (Tecsiquim, ≥99.5%), THF (Tecsiquim, >99%), DMA (Aldrich, 99.8%), acetone (Tecsiquim, ≥99.5%). All anions tested were used as sodium salts, chloride (Aldrich, 99.0%), bromide (Fluka 99.9 %), iodide, cyanide (Aldrich, 95%), sulfate (Tecsiquim, ≥99%) pyrophosphate decahydrate (Aldrich, ≥ 99.9%), nitrate (Aldrich, ≥99%), arsenate dibasic heptahydrate (Aldrich, ≥98%), acetate (Sigma-Aldrich, 99.5%),

The FT-IR spectrum was recorded in the range of 4000–600 cm^{-1} by using the standard Pike ATR cell on a Bruker Tensor 27 FT-IR spectrophotometer (Bruker Optik GmbH, Ettlingen, Germany).

Elemental analysis for C, H, and N were carried out by standard methods using a Vario Micro-Cube analyzer.

Powder X-ray diffraction (PXRD) was conducted using a Bruker D8 ADVANCE X-ray powder diffractometer (Cu-Kα, λ= 1.5418 Å) (Bruker AXS GmbH, Karlsruhe, Germany) with the 2θ range of 5–50◦. Thermogravimetric analyses were performed using a Netzsch model STA 449 F3 Jupiter equipment, under a dinitrogen atmosphere, at a heating rate of 10 ◦C min^{-1}, and from 25 to 450 ◦C. SEM-EDS. Morphological changes of **Zn-LMOF** and **Eu@Zn-LMOF** before and after the contact with fluoride solutions were evaluated by Scanning Electron Microscopy (SEM) on a JEOL (JSM-6610) microscope. For sample preparation, the specimen was dried and fixed on a stub with carbon double-stick tape and then coated with gold for 90 seconds under vacuum using a Denton IV sputtering chamber. Elemental chemical distribution analysis was performed with an energy-dispersive X-ray spectroscope QUANTAX 200 from Bruker attached to SEM.

Elemental analyses were recorded on Thermo Scientific/Flash 2000 elemental analyzer. Luminescence spectra were recorded on a Varian Cary Eclipse spectrophotometer equipped with a thermostated cell holder. UV-Vis spectra were recorded on an Agilent Cary 100 UV-VIS spectrophotometer.

Ball milling for the preparation of the **Eu@Zn-LMOF** was performed using a Planetary Micro Mill PulverisetteTM 7 Fritsch device (Idar-Oberstein, Germany)

Table S1. Crystal data and structure refinement for **Zn-LMOF.**

Empirical formula	$C_{29.20}H_{27.60}O_{14.60}Zn_3$
Formula weight	808.22
Temperature	100(2) K
Wavelength	0.71073 Å
Crystal system	Monoclinic
Space group	C2/c
Unit cell dimensions	a = 20.1166(14) Å, α= 90°.
	b = 10.6178(7) Å, β= 108.3899(12)°.
	c = 16.0756(11) Å, γ= 90°.
Volume	3258.3(4) $Å^3$
Z	4
Density (calculated)	1.648 Mg/m^3
Absorption coefficient	2.260 mm^{-1}
F(000)	1638
Crystal size	0.280 x 0.149 x 0.096 mm^3
Theta range for data collection	2.134 to 27.443°.
Index ranges	-26<=h<=26, -13<=k<=13, -20<=l<=20
Reflections collected	34640
Independent reflections	3718 [R(int) = 0.0316]
Completeness to theta = 25.242°	99.8 %
Absorption correction	None
Refinement method	Full-matrix least-squares on F^2
Data / restraints / parameters	3718 / 361 / 326
Goodness-of-fit on F^2	1.068
Final R indices [I>2sigma(I)]	R1 = 0.0456, wR2 = 0.1230
R indices (all data)	R1 = 0.0488, wR2 = 0.1257
Extinction coefficient	n/a
Largest diff. peak and hole	2.473 and -0.757 $e.Å^{-3}$

Table S2. Selected bond distances (Å) and angles (°) around Zn atoms.

Bonding	**Distance (Å)**	**Bonding**	**Angle (°)**
Zn(1)-O(5)	1.855(9)	O(5)-Zn(1)-O(1)	121.3(3)
Zn(1)-O(6A)	1.940(13)	O(5)-Zn(1)-O(4)	125.6(3)
Zn(1)-O(1)	1.945(2)	O(9A)-Zn(1)-O(4)	105.2(4)
Zn(1)-O(4)#1	1.962(2)	O(1)-Zn(1)-O(4)	108.82(12)
Zn(1)-O(6)	2.063(6)	O(5)-Zn(1)-O(9)	98.8(3)
Zn(1)-H(6)	1.97(8)	O(1)-Zn(1)-O(9)	91.45(18)
Zn(1)-H(6A)	2.10(3)	O(4)-Zn(1)-O(9)	99.8(2)
Zn(2)-O(2)	2.078(2)	O(2)-Zn(2)-O(2)	180.0
Zn(2)-O(3)	2.090(3)	O(2)-Zn(2)-O(3)	91.62(12)
		O(3)-Zn(2)-O(3)	180.00(11)

Table S3. Analytical parameters of recent luminescent materials for F^- sensing in aqueous dispersions.

Material	Stern-Volmer constant (M^{-1})	LOD (mol/L)	λ_{em} (nm)	Ref.
*Eu-MOF	-	1.14×10^{-6}	425	[1]
FS@UiO-66	-	$4.40\text{x}10^{-4}$	537	[2]
$[Cu_4I(TIPE)_3]\cdot3I$	-	$2.11\text{x}10^{-6}$	450	[3]
TMU-31	$2.53\text{x}10^{3}$	-	375	[4]
**Eu-MOF	-	$8.30\text{x}10^{-5}$	625	[5]
Eu@Zn-LMOF	$7.27\text{x}10^{3}$	$1.37\text{x}10^{-5}$	616	This work

*Eu-MOF (L= 2-aminoterephthalic acid); FS@UiO-66 (FS=Fluorescein; UiO-66 =MOF-5); TIPE = tetra(3-imidazoylphenyl) ethylene; TMU-31 (L=4,4′-(carbonylbis(azanediyl)dibenzoic acid); **Eu-MOF (L= 5-boronisophthalic acid)

[1] H. Che, Y. Li, S. Zhang, W. Chen, X. Tian, C. Yang, L. Lu, Z. Zhou and Y. Nie, *Sens. Act. B Chem*., 2020, **324**, 128641.
[2] X. Zhao, Y. Wang, X. Hao and W. Liu, *Appl. Surf. Sci*., 2017, **402**, 129-135.
[3] H. Chen, P. X. Liu, S. P. Zhuo, X. Meng, Z. Y. Zhou and H. N. Wang, *Inorg. Chem. Commun*., 2016, **63**, 69-73.
[4] M. Sharafizadeh, J. Mokhtari, H. Saeidian and Z. Mirjafary, *Environ. Sci. Pollut. Res. Int.*, 2020, **27**, 25132-25139.
[5] Z. R. Yang, M. M. Wang, X. S. Wang and X. B. Yin, *Anal. Chem*., 2017, **89**, 1930-1936.

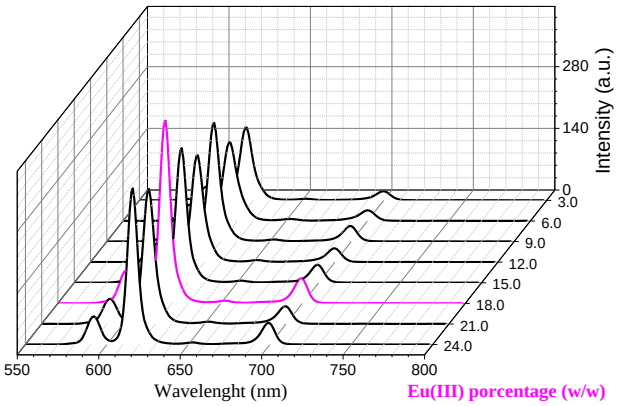

Fig. S1. Emission spectra for **$Eu_{3\text{-}24\%}$@Zn-LMOF** (λ_{ex}= 260 nm).

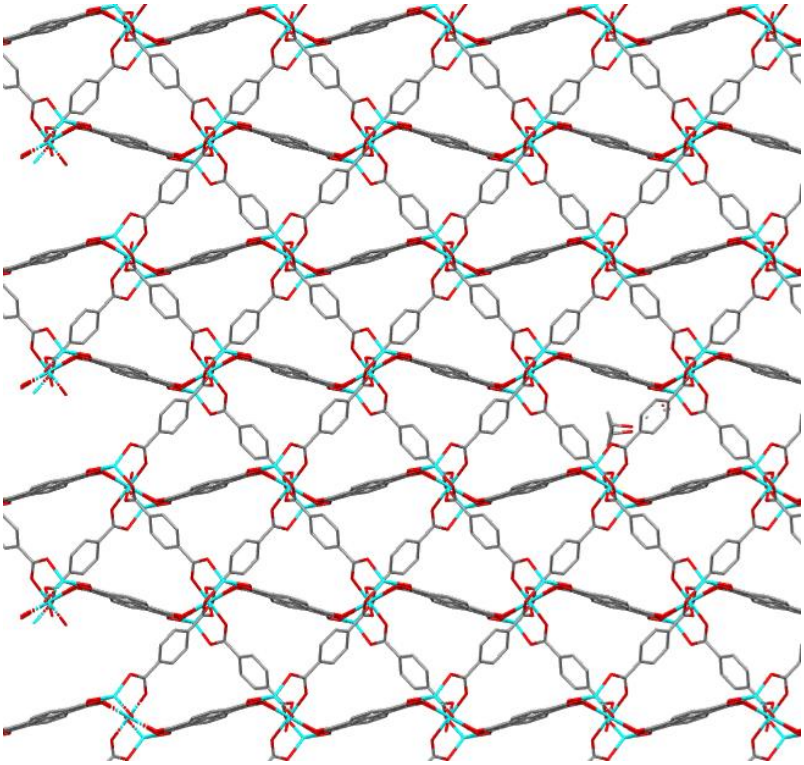

Fig. S2. The 3D diagram from crystal structure of **Zn-LMOF**.

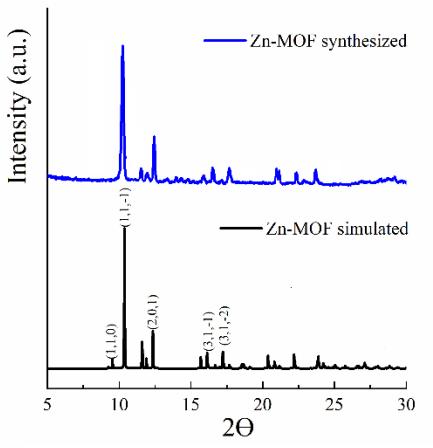

Fig. S3. Simulated and experimental powder X-ray diffraction patterns of **Zn-LMOF**.

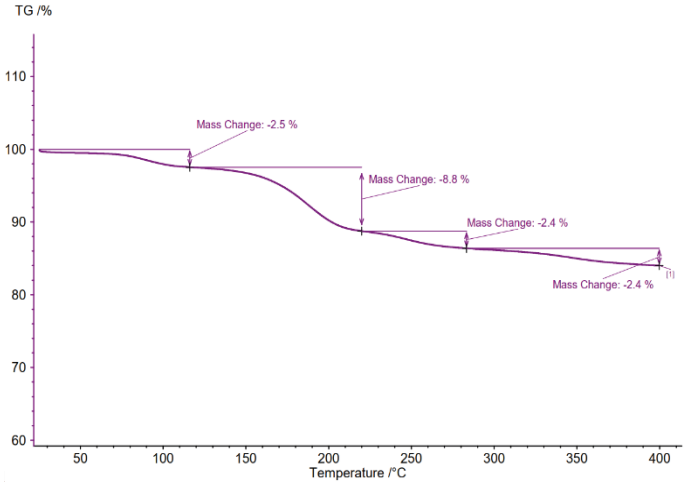

Fig. S4. TGA curve of **Zn-LMOF**

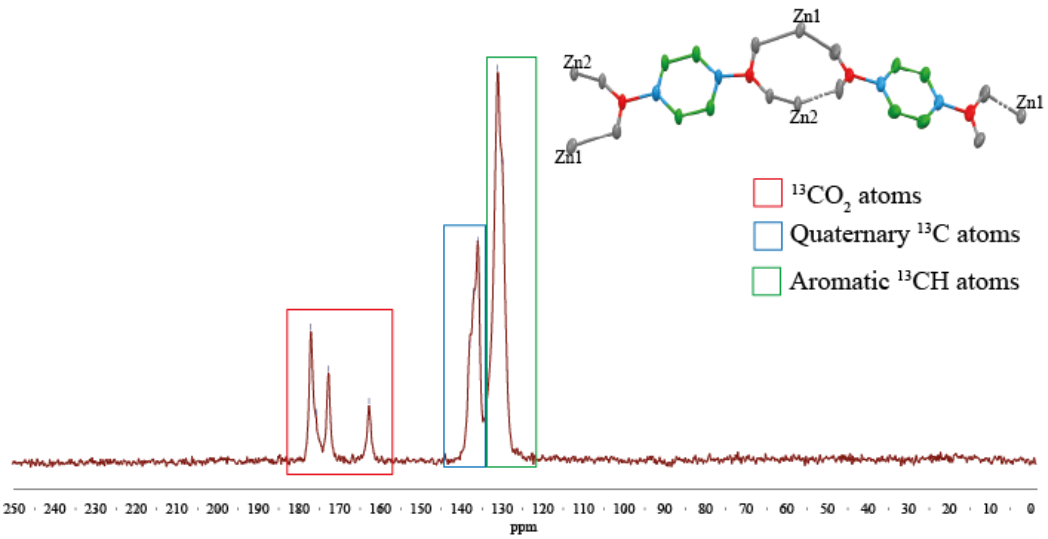

Fig. S5. ^{13}C ss-CPMAS NMR (spinning rate at 8 kHz) spectrum for **Zn-LMOF** and the asymmetric unit from the crystal structure (above). Solvent molecules are omitted for clarity.

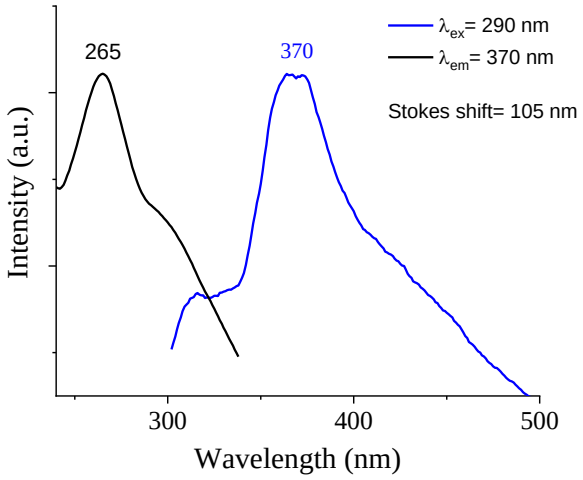

Fig. S6. Solid-state excitation (black) and emission (blue) spectra of **Zn-LMOF** at room temperature.

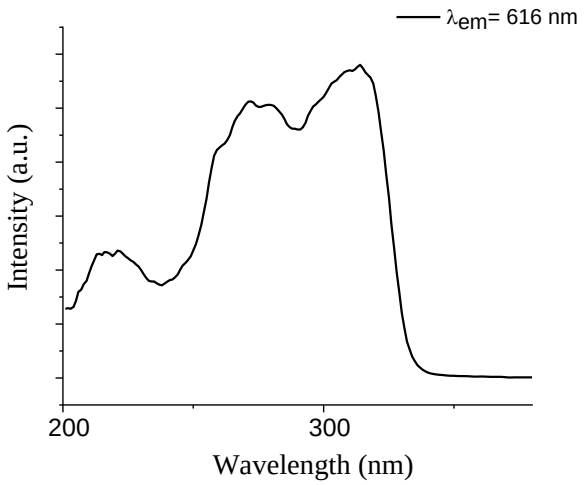

Fig. S7. Excitation spectrum of **Eu@Zn-LMOF** at room temperature by monitoring the Eu(III) ions (λ_{em}= 616 nm).

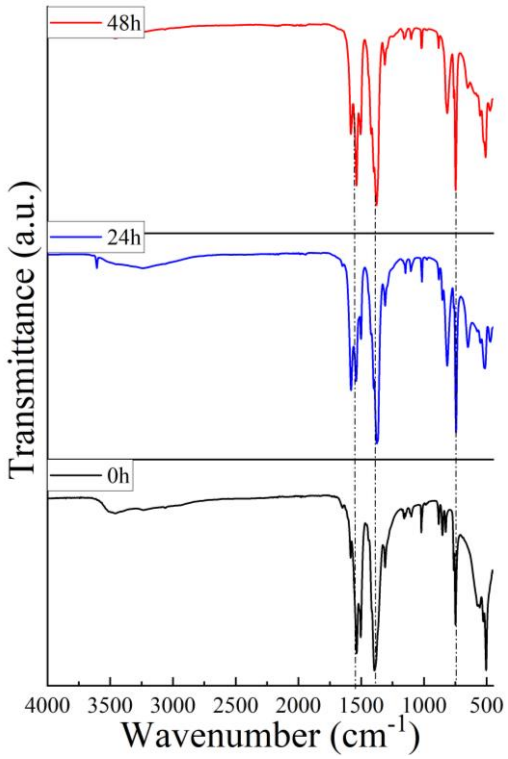

Fig. S8. ATR-FTIR spectra to assess the **Eu@Zn-MOF** hydrostability.

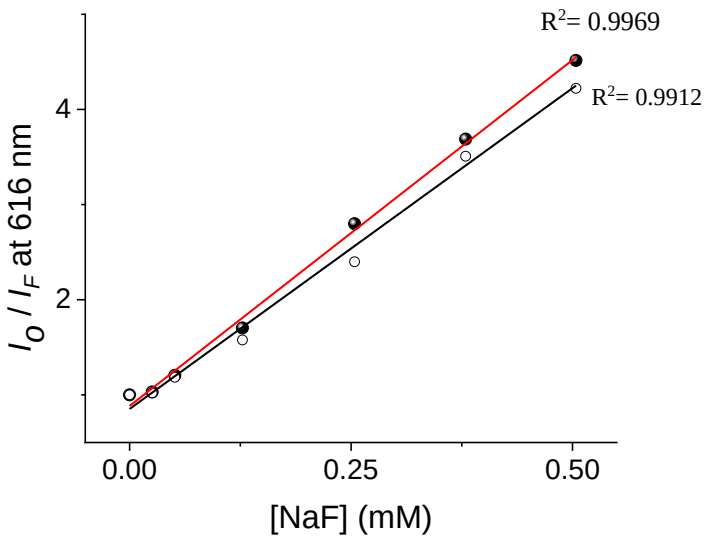

Fig. S9. Calibration curves with linear fit at 616 nm (λ_{ex}= 260 nm) of **Eu@Zn-LMOF** dispersed in EtOH-H_2O (v/v, 8/2) by adding F^- ions with (○) and without (●) interfering anions (Cl^-, Br^-, I^-, NO_3^-, AcO^-, $H_2PO_4^-$, $H_3P_2O_7^-$, and SO_4^{2-}; [X^-]= 1.0 mM each one).

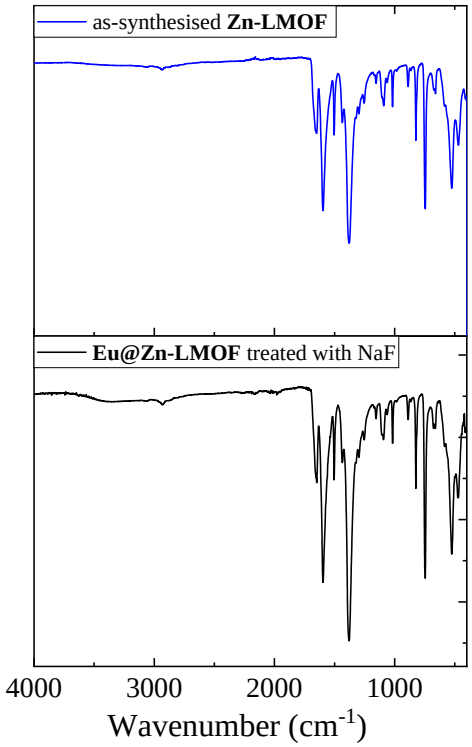

Fig. S10. IR spectra of as-synthesised **Zn-LMOF** and, **Eu@Zn-LMOF** treated with NaF for 12 h.

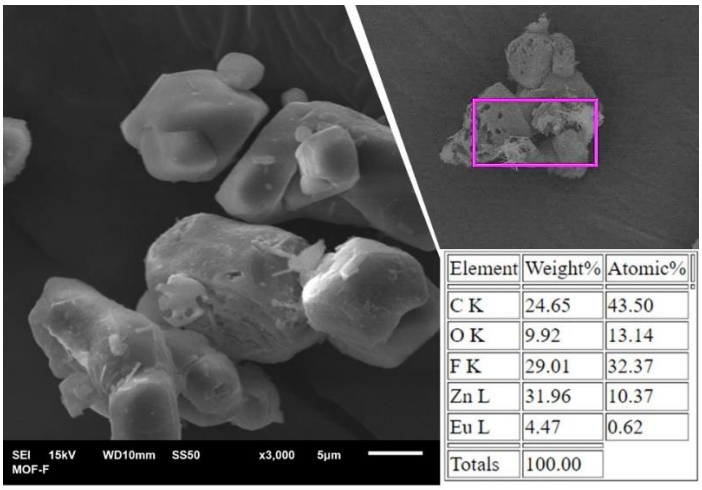

Element	Weight%	Atomic%
C K	24.65	43.50
O K	9.92	13.14
F K	29.01	32.37
Zn L	31.96	10.37
Eu L	4.47	0.62
Totals	100.00	

Fig. S11 SEM-EDS **Eu@Zn-LMOF** after F^- detection.